Molecular Crystals and Liquid Crystals

Publication details, including instructions for authors and subscription information:
http://www.tandfonline.com/loi/gmcl20

Liquid-Crystalline Behavior of Adducts between Pyridazine and Silver Alkylsulfonates

Tomoyuki Itaya [a], Masahiro Ichihara [b], Makiko Sugibayashi [b], Hwa-Tai Lin [b] & Kazuchika Ohta [b]

[a] Department of General Education, Nagano National College of Technology, Nagano, Japan

[b] Smart Materials Science and Technology, Department of Bioscience and Textile Technology, Interdisciplinary Graduate School of Science and Technology, Shinshu University, Ueda, Japan

Version of record first published: 22 Sep 2010

To cite this article: Tomoyuki Itaya, Masahiro Ichihara, Makiko Sugibayashi, Hwa-Tai Lin & Kazuchika Ohta (2007): Liquid-Crystalline Behavior of Adducts between Pyridazine and Silver Alkylsulfonates, Molecular Crystals and Liquid Crystals, 474:1, 29-41

To link to this article: http://dx.doi.org/10.1080/15421400701617756

Mol. Cryst. Liq. Cryst., Vol. 474, pp. 29–41, 2007

ISSN: 1542-1406 print/1563-5287 online
DOI: 10.1080/15421400701617756

Taylor & Francis
Taylor & Francis Group

Liquid-Crystalline Behavior of Adducts between Pyridazine and Silver Alkylsulfonates

Tomoyuki Itaya
Department of General Education, Nagano National College of Technology, Nagano, Japan

Masahiro Ichihara
Makiko Sugibayashi
Hwa-Tai Lin
Kazuchika Ohta
Smart Materials Science and Technology, Department of Bioscience and Textile Technology, Interdisciplinary Graduate School of Science and Technology, Shinshu University, Ueda, Japan

The silver-ion-based supramolecular adducts bearing long alkyl chains were prepared by reaction of pyridazine and silver alkylsulfonates. The-liquid crystalline behavior of the adducts was studied by differential scanning calorimetry, polarizing microscopy, temperature-dependent IR, and temperature-dependent X-ray diffraction. Each of the adducts exhibits two rectangular columnar mesophases having P2/a symmetry and has a strong tendency of parallel alignment of the alkyl chains orientating toward the surface of the glass substrate.

Keywords: liquid crystal; self-assembly; supramolecule

1. INTRODUCTION

Metal-containing liquid crystals have received attention because of anticipated unique properties resulting from their combination of metals and intrinsic liquid-crystalline properties of organic compounds [1–3]. On the other hand, supramolecular self-assembly is an efficient way to construct novel molecular architectures with potentially useful properties and functions that are absent in the individual

Address correspondence to Tomoyuki Itaya, Department of General Education, Nagano National College of Technology, Nagano, 381-8550, Japan. E-mail: itaya@ge.nagano-nct.ac.jp

components [4,5]. In particular, the metal-containing supramolecular systems obtained by a careful and appropriate choice of the metal cation, counter ion, and organic ligand are attractive materials, because they display an extensive range of properties [6–9]. However, few systems have been used as organic ion with alkyl chain as the counter anion [10,11]. Because the surfactants containing silver and lanthanide metals exhibit mesophases [12–14], the introduction of flexible alkyl chains into the metal-based supramolecular systems would be expected to modify their melting points, leading to novel liquid-crystalline materials.

Carlucci et al. reported that the self-assembly of pyridazine and silver salts gave rise to polymeric helical motifs [15]. We have prepared here new silver-containing supramolecules with long alkyl chains by reaction of pyridazine and silver alkylsulfonates. The introduction of long alkyl chains on the supramolecules has provided them with thermotropic mesomorphism. For example, the supramolecules exhibited a rectangular columnar mesophase (P2/a). Herein we report on the liquid-crystalline properties of the supramolecular adducts bearing long alkyl chains (Cn-Pyda) obtained by reaction of pyridazine and silver alkylsulfonates.

2. EXPERIMENTAL

2.1. Materials

Pyridazine (Pyda) was purchased from Tokyo Kasei (Tokyo) and used without further purification. Silver alkylsulfonates (silver decylsulfonate, silver dodecylsulfonate, silver tetradecylsulfonate, and silver hexadecylsulfonate) were prepared from the corresponding sodium alkylsulfonates and $AgNO_3$ [16].

The synthetic route for Cn-Pyda (n = 10–18) is shown in Scheme 1. Preparation of the representative C16-Pyda derivative was as follows. A DMSO solution (1 mL) of Pyda (0.050 g, 6.2×10^{-4} mol) was added to a

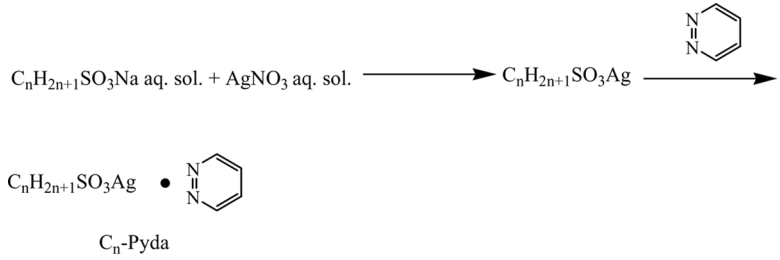

SCHEME 1 Synthetic route for Cn-Pyda.

DMSO solution (3 mL) of silver hexadecylsulfonate (0.26 g, 6.2×10^{-4} mol), and then the mixture was allowed to stand for 3 h at room temperature. The resulting white crystals (C16-Pyda) were separated by filtration to give 0.19 g in 62% yield. The other Cn-Pyda crystals were prepared in the same manner.

Elemental analysis (%) found (calc.): C10-Pyda = $C_{14}H_{25}N_2AgO_3S$: C, 40.98 (41.08); H, 6.11 (6.16); N, 6.70 (6.84). C12-Pyda = $C_{16}H_{29}N_2AgO_3S$: C, 43.78 (43.94); H, 6.58 (6.68); N, 6.25 (6.40). C14-Pyda = $C_{18}H_{33}N_2AgO_3S$: C, 46.28 (46.45); H, 7.10 (7.15); N, 5.71 (6.02). C16-Pyda = $C_{20}H_{37}N_2AgO_3S$: C, 48.38 (48.68); H, 7.58 (7.56); N, 5.42 (5.68). C18-Pyda = $C_{22}H_{41}N_2AgO_3S$: C, 51.01 (51.06); H, 7.95 (7.98); N, 5.32 (5.41).

2.2. Measurements

The samples (Cn-Pyda) were identified by elemental analysis (Perkin-Elmer elemental analyzer 2400). The phase-transition behavior of the samples was observed with a polarizing microscope, Olympus BH-2, equipped with a heating plate controlled by a thermoregulator (Mettler FP82HT hot stage, Mettler FP90 central processor), and measured with a differential scanning calorimeter, Shimazu DSC-50. Temperature-dependent X-ray diffraction measurements were performed with Cu-Kα radiation by using a Rigaku RAD X-ray diffractometer equipped with a handmade heating plate [17] controlled by a thermoregulator. Temperature-dependent IR spectra were measured by a Nicolet Nexsus 670 spectrophotometer equipped with a heating plate controlled by a thermoregulator (Mettler FP82HT hot stage, Mettler FP90 central processor).

3. RESULTS AND DISSCUSSION

3.1. Preparation of Cn-Pyda

The reaction of pyridazine (Pyda) and silver alkylsulfonate in Dimethylsulfoxide (DMSO) gave white crystalline solids (Cn-Pyda). The coordination bonding of pyridazine and Ag^+ was confirmed by FT-IR spectra. From elemental analysis, the stoichiometry of Cn-Pyda was shown to be Pyda–silver alkylsulfonate = 1:1, confirming that pyridazine and silver alkylsulfonate form a 1:1 adduct.

3.2. Phase-Transition Behavior of Cn-Pyda

The phase-transition sequences of Cn-Pyda established by differential scanning calorimetry (DSC) measurements, and polarizing microscopic

TABLE 1 Phase-Transition Temperatures and Enthalpy Changes of Cn-Pyda (n = 10, 12, 14, 16, and 18)

Compoud	Phase $\xrightarrow{\text{T (°C) } \Delta\text{[H (KJ/sol)]}}$ Phase							
C_{10}-Pyda	Cr	122.3 [43.3]	M_1	142.2 [0.624]	M_2	*ca.* 202	Decomp.	
C_{12}-Pyda	Cr	123.3 [55.6]	M_1	144.0 [0.310]	M_2	*ca.* 211	Decomp.	
C_{14}-Pyda	Cr	124.7 [71.2]	M_1	141.9 [0.324]	M_2	*ca.* 218	Decomp.	
C_{16}-Pyda	Cr	124.7 [71.4]	M_1	144.1 [0.597]	M_2	*ca.* 215	Decomp.	
C_{18}-Pyda	Cr	125.5 [76.8]	M_1	135.9 [0.788]	M_2	*ca.* 203	Decomp.	

Note. Phase nomenclature: Cr = crystal and M = mesophase. M_1 = rectagular columnar mesopahse Col_{r1} (P2/a). M_2 = rectagular columnar mesopahse Col_{r2} (P2/a).

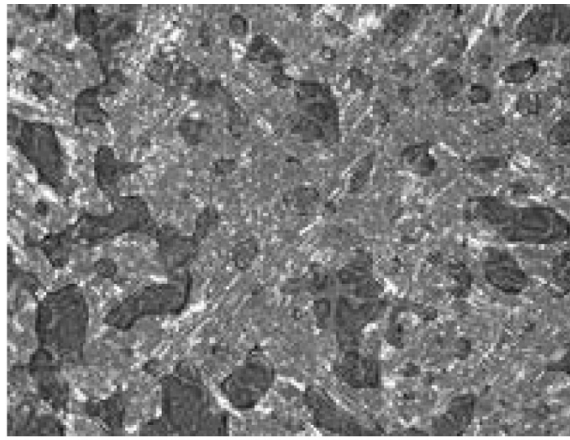

(a)

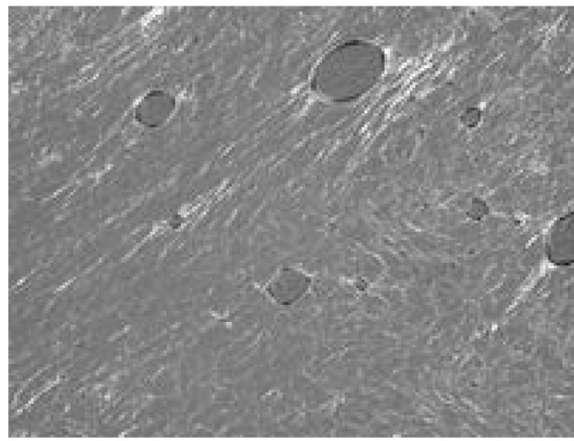

(b)

FIGURE 1 Photomicrographs of C18-Pyda at 130°C (top) and 150°C (bottom).

observations are summarized in Table 1. The temperature-dependent IR spectra were also measured to gain the information on the conformation of alkyl chains. Because each of them shows the same transition sequence, a representative C18-Pyda is described here.

When the virgin crystals of Cr were heated from room temperature, a phase transition from Cr to a mesophase M_1 could be observed at 125.5°C. Figure 1a shows a photomicrograph of the M_1 mesophase at 130°C. It was waxy and soft with birefringence. On further heating, it could be observed only by DSC that the M_1 phase transformed into

another mesophase, M_2, at 135.9°C. No discernible changes of the texture were observed by the polarizing optical microscope, which is attributed to a very small enthalpy change for the M_1–M_2 phase transition. Figure 1b shows a photomicrograph of the M_2 mesophase at 150°C. This M_2 mesophase showed more fluidity with birefringence than the M_1 mesophase. On further heating, the M_2 phase decomposed at ca. 203°C. Thus, both M_1 and M_2 phases were very soft and waxy and exhibited birefringence under the polarizing microscope. Because the sample decomposed before clearing into an isotropic liquid, it was impossible to observe the natural textures and characterize the mesophases from the natural textures.

Figure 2 shows the IR spectra of C18-Pyda measured in the region from 700 cm^{-1} to 1400 cm^{-1} at room temperature, 130, and 150°C. At

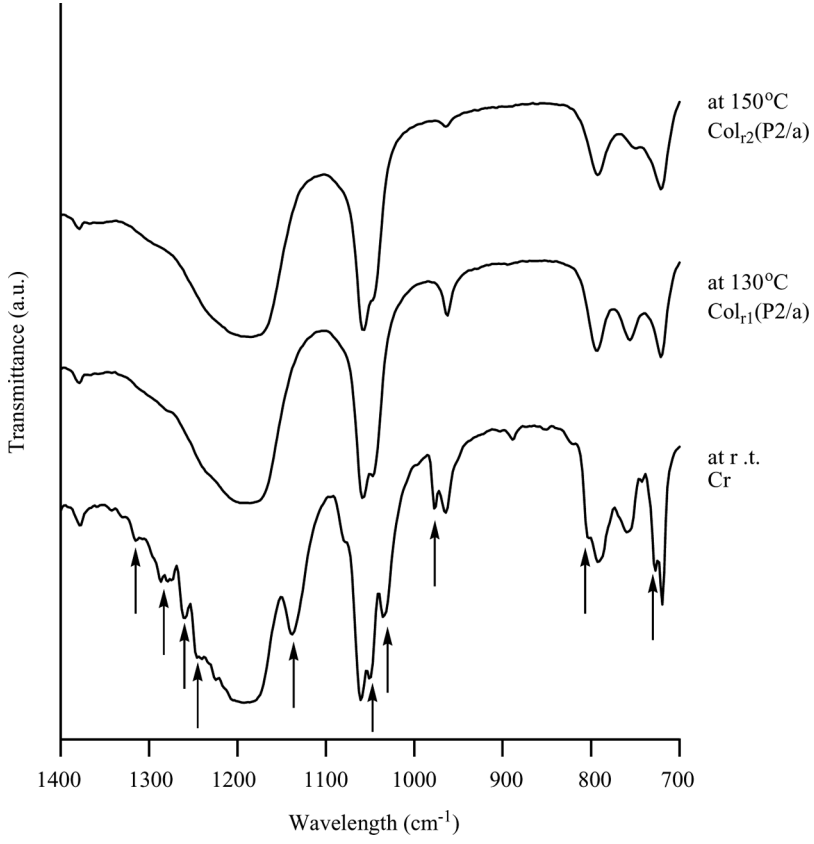

FIGURE 2 Temperature-dependent IR spectra of C18-Pyda at room temperature, 130°C and 150°C.

room temperature, many fine structures could be observed in this region. They are assigned to band progressions of the alkyl chains indicating the trans-zigzag conformation of the alkyl chain [18]. On the other hand, at 130 and 150°C, the band progressions smeared out to show the structureless spectra. This suggests that the trans-zigzag conformation of the alkyl chains in the crystal phase (Cr) is completely destroyed by melting in the M_1 and M_2 phases [18]. It is compatible with the waxy nature and softness of these M_1 and M_2 phases. Hence, they can be regarded as mesophases.

3.3. Mesophase Structure of Cn-Pyda

The M_1 and M_2 mesophases were identified by temperature-dependent X-ray analyses. The X-ray diffraction data of all the mesophases are summarized in Table 2.

As can be seen from Table 2, the M_1 and M_2 mesophases of C18-Pyda gave many sharp reflections. Although a halo at $2\theta \fallingdotseq 20^\circ$ corresponding to the melting of long alkyl chains was not distinctly observed, the melting of alkyl chains in these phases was obvious from the waxy nature and smearing out the band progressions, as mentioned previously. This is described in detail later.

The peaks in the M_1 mesophase could be assigned as reflections from a rectangular columnar (Col_{r1}) phase. Moreover, it was clarified from the extinction rules for rectangular lattices that this Col_r mesophase has P2/a symmetry. Similarly, the M_2 mesophase could be identified as the same Col_{r2} (P2/a) phase.

Each of the M_1 and M_2 phases of the other adducts (Cn-Pyda; $n = 10$, 12, 14, and 16) could be also identified as a Col_r (P2/a) mesophase (Table 2). As can be seen from Table 2, the lattice constants a and b for these rectangular lattices for the Col_{r1} and Col_{r2} mesophases increase with increasing the alkyl chain lengths from $n = 10$ to $n = 18$. The lattice constants a and b of the Col_{r2} phase are slightly bigger than those of the Col_{r1} phase. This means that the packing of columns is somewhat looser in the higher-temperature mesophase Col_{r2} compared with the lower-temperature mesophase Col_{r1}. The very small difference between these two rectangular columnar mesophases of Col_{r1} and Col_{r2} with the same symmetry corresponds to the small enthalpy change of the phase transition from Col_{r1} to Col_{r2} (Table 1).

3.4. Model of the Col_r Mesophases

Figure 3 illustrates a structure model of the Col_{r1} and Col_{r2} mesophases of the Cn-Pyda adducts on a glass substrate. As mentioned

TABLE 2 X-ray Diffraction Data of the Cn-Pyda Adducts

Compound	Mesophase lattice constants (Å)	Spacing (Å)		Miller indices (h k l)
		Observed	Calculated	
C10-Pyda	Col_{r1} (P2/a) at 125°C	30.9	29.9	(1 1 0)
	a = 45.0	22.5	22.5	(2 0 0)
	b = 37.7	18.9	18.9	(0 2 0)
		17.2	17.4	(1 2 0)
		15.4	15.0	(3 0 0)
		11.2	11.3	(4 0 0)
		8.58	8.70	(2 4 0)
		7.94	7.99	(3 4 0)
		7.47	7.44	(1 5 0)
		6.11	6.09	(7 2 0)
		5.72	5.73	(7 3 0)
		4.42	4.42	(9 4 0)
	Col_{r2} (P2/a) at 150°C	30.9	30.9	(1 1 0)
	a = 54.8	27.4	27.4	(2 0 0)
	b = 37.3	22.8	22.1	(2 1 0)
		15.3	15.4	(2 2 0)
		13.7	13.7	(4 0 0)
		11.3	11.3	(2 3 0)
		10.2	10.3	(3 3 0)
		9.17	9.20	(1 4 0)
C12-Pyda	Col_{r1} (P2/a) at 130°C	24.8	24.8	(2 0 0)
	a = 49.6	18.6	18.6	(0 2 0)
	b = 37.3	12.6	12.4	(4 0 0)
		9.40	9.31	(0 4 0)
		8.42	8.27	(6 0 0)
		8.02	8.07	(6 1 0)
		6.37	6.39	(4 5 0)
		5.04	5.04	(9 3 0)
		4.40	4.39	(8 6 0)
		4.03	4.03	(12 2 0)
		3.60	3.61	(12 5 0)
		3.43	3.44	(11 7 0)
		3.20	3.19	(8 10 0)
	Col_{r2} (P2/a) at 150°C	29.8	29.8	(1 1 0)
	a = 50.2	25.1	25.1	(2 0 0)
	b = 37.1	17.7	17.4	(1 2 0)
		15.8	15.2	(3 1 0)
		15.1	15.2	(3 1 0)
		12.7	12.5	(4 0 0)
		11.8	11.9	(4 1 0)
		10.5	10.4	(4 2 0)
		10.1	10.0	(5 0 0)
		8.50	8.36	(6 0 0)
		6.39	6.38	(4 5 0)

(*Continued*)

TABLE 2 Continued

Compound	Mesophase lattice constants (Å)	Spacing (Å)		Miller indices (h k l)
		Observed	Calculated	
C14-Pyda	Col_{r1} (P2/a) at 130°C	28.8	28.8	(2 0 0)
	a = 57.7	23.6	23.6	(0 2 0)
	b = 47.2	20.6	21.8	(1 2 0)
		14.3	14.4	(4 0 0)
		11.0	10.9	(2 4 0)
		10.4	10.4	(5 2 0)
		9.52	9.62	(6 0 0)
		8.65	8.48	(3 5 0)
		8.17	8.21	(6 3 0)
		7.13	7.13	(8 1 0)
		6.93	6.91	(4 6 0)
		6.65	6.70	(1 7 0)
		5.36	5.32	(8 6 0)
		4.43	4.43	(7 9 0)
		4.39	4.38	(10 7 0)
	Col_{r2} (P2/a) at 150°C	34.0	34.0	(1 1 0)
	a = 57.0	28.5	28.5	(2 0 0)
	b = 42.3	21.1	21.1	(0 2 0)
		20.1	19.8	(1 2 0)
		17.2	17.3	(3 1 0)
		14.3	14.2	(4 0 0)
		14.0	14.1	(3 2 0)
		13.3	13.5	(4 1 0)
		11.6	11.4	(5 0 0)
		10.5	10.6	(0 4 0)
		9.58	9.49	(6 0 0)
		8.70	8.66	(6 2 0)
		8.40	8.37	(1 5 0)
C16-Pyda	Col_{r1} (P2/a) at 130°C	32.0	32.0	(2 0 0)
	a = 64.0	23.9	23.9	(0 2 0)
	b = 47.7	22.5	22.4	(1 2 0)
		15.8	15.9	(3 2 0)
		11.9	11.9	(0 4 0)
		11.6	11.7	(1 4 0)
		11.3	11.3	(4 3 0)
		10.5	10.4	(3 4 0)
		8.28	8.20	(4 5 0)
		7.88	7.89	(8 1 0)
		7.56	7.58	(8 2 0)
		6.87	6.81	(9 2 0)
		6.32	6.34	(10 1 0)
		5.67	5.65	(11 2 0)
		4.65	4.65	(12 5 0)

(*Continued*)

TABLE 2 Continued

Compound	Mesophase lattice constants (Å)	Spacing (Å)		Miller indices (h k l)
		Observed	Calculated	
		4.44	4.43	(12 6 0)
		3.95	3.95	(2 12 0)
C16-Pyda	Col_{r2} (P2/a) at 150°C	38.0	38.0	(1 1 0)
	a = 64.9	32.5	32.5	(2 0 0)
	b = 47.0	23.7	23.5	(0 2 0)
		19.4	19.7	(3 1 0)
		15.8	15.9	(3 2 0)
		13.0	13.0	(5 0 0)
		11.7	11.7	(0 4 0)
		10.6	10.5	(6 1 0)
		9.77	9.83	(6 2 0)
		9.40	9.30	(1 5 0)
		7.96	7.96	(6 4 0)
C18-Pyda	Col_{r1} (P2/a) at 130°C	34.5	33.8	(2 0 0)
	a = 67.7	26.3	26.0	(0 2 0)
	b = 51.9	23.9	24.2	(1 2 0)
		22.4	22.6	(3 0 0)
		17.4	17.0	(3 2 0)
		15.0	15.4	(2 3 0)
		13.1	13.1	(5 1 0)
		12.1	12.1	(2 4 0)
		11.5	11.3	(6 0 0)
		10.5	10.3	(6 2 0)
		9.09	9.06	(7 2 0)
		8.63	8.66	(0 6 0)
		8.31	8.35	(8 1 0)
		8.13	8.08	(3 6 0)
		7.01	7.05	(3 7 0)
		6.09	6.09	(9 5 0)
		5.83	5.85	(5 8 0)
		4.44	4.44	(8 10 0)
		4.44	4.44	(15 2 0)
		4.31	4.32	(1 12 0)
		3.85	3.85	(8 12 0)
		3.07	3.08	(14 13 0)
		2.71	2.75	(15 15 0)
C18-Pyda	Col_{r2} (P2/a) at 150°C	34.2	34.2	(2 0 0)
	a = 68.4	25.8	25.8	(0 2 0)
	b = 51.6	20.9	20.9	(3 1 0)
		17.2	17.1	(4 0 0)
		14.1	14.3	(4 2 0)
		12.9	12.9	(0 4 0)
		10.3	10.3	(4 4 0)

(*Continued*)

TABLE 2 Continued

Compound	Mesophase lattice constants (Å)	Spacing (Å)		Miller indices (h k l)
		Observed	Calculated	
		8.61	8.60	(0 6 0)
		7.38	7.33	(1 7 0)
		6.57	6.59	(8 5 0)
		5.97	6.04	(4 8 0)
		4.33	4.34	(6 11 0)
		3.44	3.44	(1 15 0)
		3.23	3.23	(14 12 0)
		3.04	3.03	(1 17 0)
		2.72	2.72	(8 18 0)
		2.58	2.58	(0 20 0)
		2.35	2.35	(20 16 0)

in the introduction, Carlucci et al. reported that the self-assembly of pyridazine and silver salts gave rise to polymeric helical motifs, in which pyridazine and Ag^+ formed a rigid skeletone [15]. The Cn-Pyda adducts also seem to have a rigid skeleton like a column, although details of the exact coordination structure of pyridazine and Ag^+ ion remain unclear. Alkylsulfonate anions bound to Ag^+ ions on the rigid skeleton modify its melting point to reveal liquid-crystalline mesophases. We tentatively think that the oval columnar adducts surrounded by the alkyl chains assemble parallel to the surface of glass substrate, as illustrated in Figure 3. It is noteworthy that a diffuse halo at $2\theta \fallingdotseq 20^\circ$ corresponding to the melting of alkyl chains could not be observed distinctly in the present X-ray diffraction patterns of the Col_{r1} and Col_{r2} mesophases for Cn-Pyda, as mentioned previously. Similar disappearance of halo of the poly(3-alkylthiophene) π-conjugated polymers have been reported. It originated from the alignment of the polymers on substrate, with the alkyl side chains

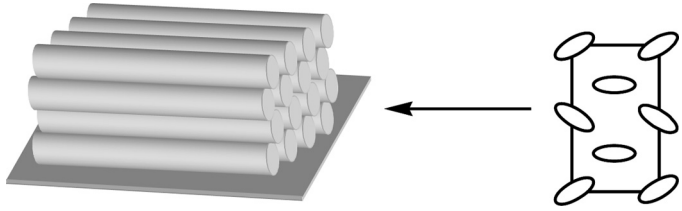

FIGURE 3 Tentative structure on a glass substrate of the rectangular columnar mesophase having P2/a symmetry of Cn-Pyda.

oriented toward the surface of the substrate [19]. Therefore, the Cn-Pyda adducts may also have a strong tendency of the alkyl chains orientating toward the surface of the glass substrate. As pointed out by Ujiie, ionic liquid crystals themselves work as a surface treatment reagent like a silane coupling reagent [20]. The present ionic liquid crystal containing silver ions (Cn-Pyda) may also work as a surface treatment reagent to show this spontaneous alignment as illustrated in Figure 3.

4. CONCLUSION

In this study, we have prepared novel adducts of Cn-Pyda (n = 10–18) between pyridazine (Pyda) and silver alkylsulfonate. The stoichiometry of Cn-Pyda was confirmed from the elemental analysis; pyridazine and silver alkylsulfonate form a 1:1 adduct. Very interestingly, each of the adducts exhibits two rectangular columnar mesophases having P2/a symmetry. In the mesophases, Cn-Pyda has a strong tendency of spontaneous alinment of the alkyl chains orientating toward the surface of the glass substrate. Introduction of the alkyl chains into metal-containing supramolecular systems can provide them with thermotropic mesomorphism and will open new possibilities for the constructions of metallomesogens.

ACKNOWLEDGMENT

This work was partially supported by Grants-in-Aid for Scientific Research (Nos. 13750819 and 19022o11) from the Ministry of Education, Culture, Sports, Science and Technology, Japan.

REFERENCES

[1] Serrano, J. L. (1996). *Metallomesoges: Synthesis, Properties and Applications*, VCH: Weinheim.
[2] Neve, F. (1996). *Adv. Mater.*, *8*, 277.
[3] Binnemans, K. (2005). *Chem. Rev.*, *105*, 4148.
[4] Vogtle, F. (1991). *Supramolecular Chemistry*, Wiley: Chichester.
[5] Lehn, J. M. (1995). *Supramolecular Chemistry: Concepts and Perspectives*, VCH: Weinheim.
[6] Robson, R., et al. (1992). Crystal engineering of novel materials composed of infinite two- and three-dimensional frameworks. In: *Supramolecular Architecture: Synthetic Control in Thin Films and Solids*, Thomas, B. (Ed.), ACS Publications: Washington, DC, p. 256.
[7] Yaghi, O. M., Li, H., Davis, C., Richardson, D., & Groy, T. L. (1998). *Acc. Chem. Res.*, *31*, 474.
[8] Kitagawa, S. & Kondo, M. (1998). *Bull. Chem. Soc. Jpn.*, *71*, 1739.

[9] Glanneschi, N. C., Masar III, M. S., Mirkin, C. A. (2005). *Acc. Chem. Res.*, *38*, 825.
[10] El-ghayoury, A., Douce, L., Skoulios, A., & Ziessel, R. (1998). *Angew. Chem. Int. Ed.*, *37*, 1255.
[11] Itaya, T. (2004). *Kobunshi Ronbunshu*, *61*, 323.
[12] Binnemans, K., Deun, R. V., Thijs, B., Vanwelkenhuysen, I., & Geuens, I. (2004). *Chem. Mater.*, *16*, 2021.
[13] Binnemans, K. & Gorller-Walrand, C. (2002). *Chem. Rev.*, *102*, 2303.
[14] Rout, D. K. & Choudhary, R. N. P. (1989). *Liq. Cryst.*, *4*, 393.
[15] Carlucci, L., Ciani, G., Proserpio, D. M., & Sironi, A. (1998). *Inorg. Chem.*, *37*, 5941.
[16] Itaya, T. & Inoue, K. (2000). *Kobunshi Ronbunshu*, *57*, 665.
[17] (a) Ema, H. (1988). MSc Thesis, Shinshu University, Japan, Chap. 7; (b) Hasebe, H. (1991). MSc Thesis, Shinshu University, Japan, Chap. 5.
[18] (a) Imamura, K., Shimizu, K., & Nogami, T. (1986). *Bull. Chem. Soc. Jpn.*, *59*, 2699; (b) Shimizu, J., Imamura, K., Nogami, T., & Mikawa, H. (1986). *Bull. Chem. Soc. Jpn.*, *59*, 3367; (c) Terada, T., Nogami, T., & Shirota, Y. (1989). *Bull. Chem. Soc. Jpn.*, *62*, 5.
[19] Yamamoto, T., Kokubo, H., Kobashi, M., & Sakai, Y. (2004). *Chem. Mater.*, *16*, 4616; (b) Kokubo, H., Sato, T., & Yamamoto, T. (2005). *Mol. Cryst. Liq. Cryst.*, *432*, 83.
[20] Ujiie, S. (1999). *Ekisho*, *3*, 85.